Line edge roughness measurement on vertical sidewall for reference metrology using a metrological tilting atomic force microscope

Ryosuke Kizu
Ichiko Misumi
Akiko Hirai
Satoshi Gonda

Line edge roughness measurement on vertical sidewall for reference metrology using a metrological tilting atomic force microscope

Ryosuke Kizu, * **Ichiko Misumi, Akiko Hirai, and Satoshi Gonda**
National Metrology Institute of Japan, National Institute of Advanced Industrial Science and Technology, Tsukuba, Japan

Abstract. Line edge roughness (LER) measurement is one of the metrology challenges for three-dimensional device structures, and LER reference metrology is important for reliable LER measurements. For the purpose of LER reference metrology, we developed an LER measurement technique that can analyze LER distribution along the height of a line pattern, with high resolution and repeatability. A high-resolution atomic force microscopy (AFM) image of a vertical sidewall of a line pattern was obtained using a metrological tilting-AFM, which offers SI-traceable dimensional measurements. The tilting-tip was controlled with an inclined servo axis, and it scans the vertical sidewall along a line pattern with a high sampling density to enable an analysis of the LER height distribution at the sidewall. A horizontal cross-section of the sidewall shows sidewall roughness with sub-nm resolution. Power spectral density (PSD) analysis of the sidewall profile showed that the PSD noise in the high-frequency region was several orders of magnitude lower than the noise of typical scanning electron microscopy methods. AFM measurements were sequentially repeated three times to evaluate the repeatability of the LER measurement; results indicated a high repeatability of 0.07 nm evaluated as a standard deviation of LER at each height. © *The Authors. Published by SPIE under a Creative Commons Attribution 4.0 Unported License. Distribution or reproduction of this work in whole or in part requires full attribution of the original publication, including its DOI.* [DOI: 10.1117/1.JMM.19.1.014003]

1 Introduction

The line edge roughness (LER) of a line pattern is an important dimensional parameter and should be measured precisely for the fabrication of semiconductor devices. Critical-dimension scanning electron microscopes (CD-SEM) are commonly used as LER metrology tools in the fabrication process because of their high throughput and reasonably good resolution. However, the use of CD-SEMs to provide absolute LER measurements at the sub-nm scale is unreliable because of the difficulty of line-edge determination[1] and the random noise in the high-frequency region.[2–4] As the dimensions of semiconductor devices continue to decrease, the horizontal resolution of the SEM becomes insufficient. In addition, CD-SEM provides a top-view (two-dimensional) metrology and cannot be used to measure a three-dimensional (3-D) profile of the vertical sidewall of a line pattern. Moreover, the sample damage or contamination caused by electron-beam exposure cannot be ignored for LER measurements at the single-nm scale. LER measurements done only by CD-SEM are no longer reliable when considering recent lithography advances; the determination of a new LER metrology method thus poses a new metrology challenge for 3-D device structures.[5]

Two LER reference metrology techniques that offer a high-resolution sidewall profile and provide a reference standard[6] to evaluate CD-SEM have been proposed, including the use of transmission electron microscopy (TEM)[7–10] and atomic force microscopy (AFM).[11–13] The TEM technique involves preparing the sample using a focused ion beam instrument so that the


*Address all correspondence to Ryosuke Kizu, E-mail: r-kizu@aist.go.jp

horizontally sliced image of the line patterns, i.e., projected onto the xy plane, can be measured by TEM.[7–10] This technique allows for higher resolution due to less noise when compared with the conventional SEM technique, the simultaneous measurement of multiple line patterns in a field-of-view, and the analysis of actual devices. However, it is a destructive metrology technique. The AFM technique involves the use of a special probe control with two-axis force sensitivity, which enables the AFM tip to scan the vertical sidewall, known as CD-AFM (using a flared tip) and tilting-AFM.[11–15] This technique provides high resolution, is nondestructive, and provides a 3-D sidewall profile. Complementary use of the TEM and AFM techniques is preferable for various purposes of the LER reference metrology.

Although these AFM techniques utilize a probe tip that inhibits usage in dense line patterns and provide lower throughput than the SEM technique, nondestructive AFM metrology techniques could be used to calibrate the LER reference standards used for the evaluation of CD-SEM's LER measurement performance. Furthermore, CD-AFM using a flared tip has been shown to measure the vertical sidewall of a line pattern and has been used for CD measurement, the most basic dimensional parameter of the line pattern, in the semiconductor industry. However, the large tip used (typically, tens of nanometers) limits the resolution when measuring surface roughness.[3,14,15] As the tilting-AFM techniques use a normal sharp tip, the sidewall roughness can be measured with high resolution, although only one side of the line pattern can be measured per measurement. As such, several studies have investigated sidewall roughness measurements using the tilting-AFM technique[16–20] by mostly evaluating sidewall surface roughness expressed in standard deviation of the distance between each point and least-squared plane of point cloud at the sidewall, while the height information is ignored. The LER distribution along the height (i.e., precise height distribution of LER in the line pattern's sidewall) is beneficial for the evaluation of advanced devices with sidewall roughness dependent on height,[21] although special data processing is necessary. Tip scanning along a line pattern, as shown in Fig. 1(a), can more effectively measure the LER than tip scanning across a line pattern [shown in Fig. 1(b)] owing to the less thermal drift error in the AFM that causes a relative position error between each fast-scan profile. To scan a vertical sidewall along a line pattern, the tilting-tip can be controlled with the servo axis inclined by θ_p during the scan on the vertical sidewall. However, the movement of the tilting-tip is restricted within the inclined servo axis, as shown in Fig. 2(a), making it difficult to scan at a fixed height. Thus, the height of data points in a fast-scan profile varies depending on the sidewall asperity, as shown in Fig. 2(b). A high sampling density and appropriate data processing are therefore necessary to calculate the LER height distribution. Fouchier et al. measured the sidewall profile with a pixel size of about 5.5 and 3.9 nm in the vertical and horizontal directions, respectively, using a tilting-AFM (sample-tilting type) and interpolated the data points using a grid in the xz plane to enable the calculation of LER distribution along the height.[13] To measure the LER in high resolution, i.e., to evaluate the LER up to the high-frequency region, a high sampling density is necessary in both fast and slow scans. In addition, the internal scale of the AFM instrument and the repeatability of the LER measurement should be evaluated for LER reference metrology.

We developed a metrological tilting-AFM (tilting-mAFM) to measure the dimensional parameters of nanoscale 3-D structures.[22,23] The probe-tip displacement is precisely measured
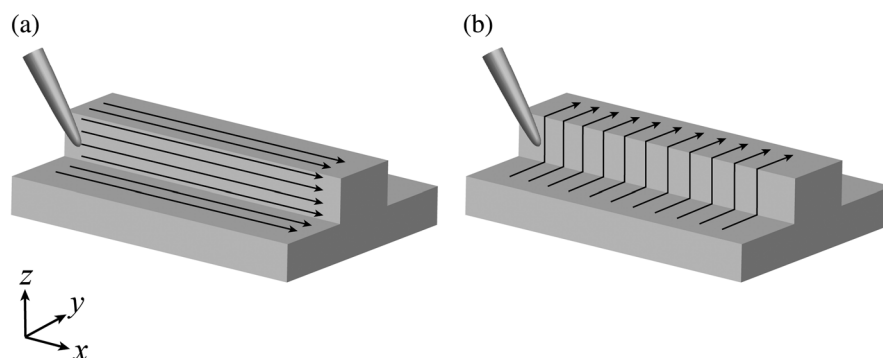
Fig. 1 Fast scan (a) along and (b) across line pattern using tilting-TiP.
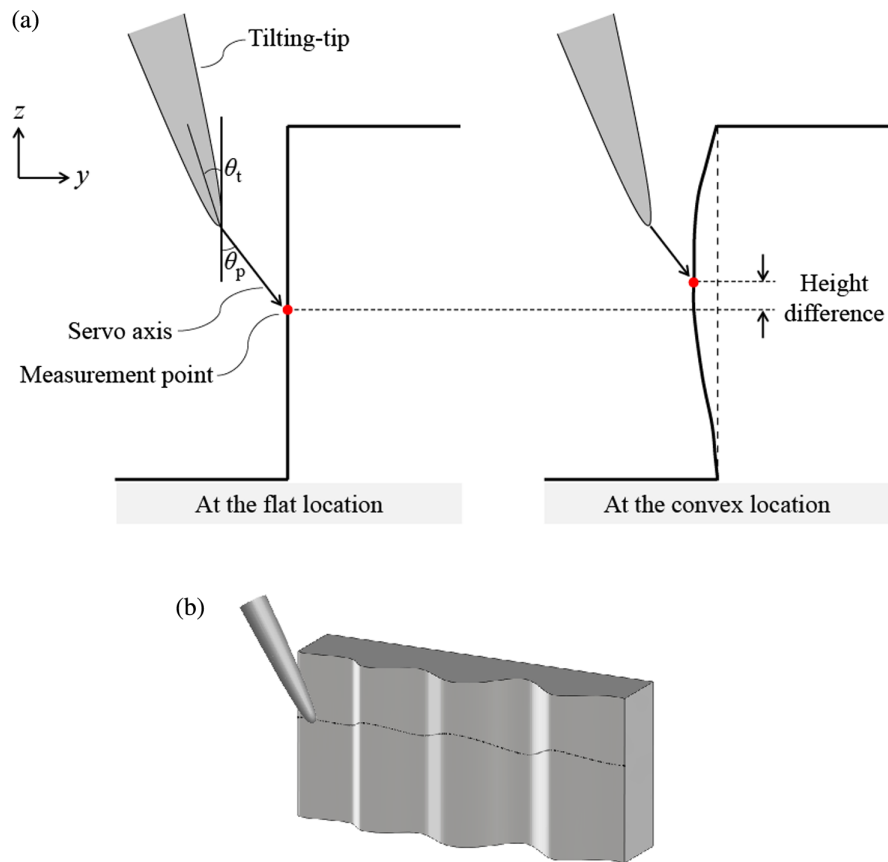
Fig. 2 (a) Tilting-tip inclined by θ_t and controlled with the servo axis inclined by θ_p. (b) Heights of data points in a fast-scan profile vary depending on the sidewall asperity.

in the x, y, and z axes using high-resolution laser interferometers. As the frequency of the laser source is calibrated using an iodine-stabilized He–Ne laser, the internal scale of the tilting-mAFM is traceable to the SI unit of length. This study aims to measure the sidewall surface of a line pattern with high sampling density ($\geq 1 \ nm^{-2}$) and rearrange the AFM data to obtain the LER height distribution. We demonstrated the LER measurement of the line pattern and scaling analysis, such as power spectral density (PSD) and height–height correlation function (HHCF).[24,25] In addition, the resolution of the sidewall profile measurement and the repeatability of LER measurement for reference metrology is evaluated.

2 Experimental Setup

The tilting-mAFM was used to perform LER measurement of a nanoscale line pattern. An OMCL-AC200TS (Olympus Corp.) cantilever probe was used. The tip-tilting-angle (θ_t) and inclining angle of the servo axis (θ_p) were 14 deg and 30 deg, respectively, as described in Sec. 3.2 in Ref. 22. The θ_p was empirically determined considering the servo-control stability and data density on the sidewall, as described in the Appendix. The AFM scanner was closed-loop controlled using the signals from the laser interferometers for the x and y axes and from the AFM signal for the z axis. In the inclined servo-axis control, tip position in the y axis was controlled using the signal proportional to the z axis displacement as well as the y-axis displacement. The inclined servo-axis control indirectly controlled the y-axis scanner based on the AFM signal, enabling the inclined servo-axis control.

The stability of scanning the sidewall along the line pattern was evaluated for repeatability in advance following the procedure described in Sec. 4.2 in Ref. 22, i.e., the stability was evaluated separately from the surface roughness by repeatedly measuring the sidewall profiles at the same

Table 1 Repeatability of the fast scan in the x, y, and z coordinates on the sidewall and horizontal surface.

|	x (nm)	y (nm)	z (nm)
Sidewall surface	0.17	0.19	0.23
Horizontal surface	0.18	0.14	0.09

location and evaluating the standard deviation of the coordinates of the data points. An Si line pattern ∼200 nm in both height and width, fabricated by NTT Advanced Technology Corp. using electron-beam lithography, was used for evaluation. Ten fast-scan profiles were measured at the same location on the sidewall surface along the line pattern for over 2000 nm with 1000 data points per fast-scan profile. A point of first index was selected from the first fast-scan profile; the standard deviation of the x, y, and z coordinates of 10 points with same index was then calculated. The standard deviations were calculated for the consecutive 999 indices in the same way. Thus, the repeatability was evaluated as the average of the 1000 standard deviations. The same procedure was executed for the 1000 points at the horizontal surface of the line pattern, too. The evaluated repeatability of the scanned profiles in the x, y, and z coordinates indicates that the tip scanning along the line pattern has sub-nm repeatability, as shown in Table 1.

One side of the line pattern was then measured by the tilting-mAFM with the following parameters: 500 lines, each with 2000 points for 2000 nm along the x axis or longitudinal direction of the line pattern (fast axis) and 180 nm along the y axis or linewidth direction (slow axis). This satisfies the high sampling density (≥ 1 nm^{-2}) in the sidewall of the line pattern. A single measurement spanned ∼48 min. LER results are analyzed in Sec. 3, where the top and bottom surfaces are defined, and the AFM data (point clouds) are partitioned in the height direction. The point clouds of each partition represent the horizontal cross-section of the line pattern at each height.

3 Results and Discussion

3.1 Sidewall Measurement Results and Analysis of LER Height Distribution

As shown in Fig. 3, the AFM image expressed as point clouds showed vertical streaks on the sidewall, likely formed owing to the fabrication process of the Si line pattern. The point clouds of the AFM data were analyzed to calculate the LER height distribution. Rough LER (or sidewall roughness) can be estimated from the projection of one fast-scan profile onto the xy plane. However, the height (z coordinate) of the fast-scan profile varies depending on the sidewall asperity, as was shown in Fig. 2(b). The height variation of one fast-scan profile extracted from the data shown in Fig. 3 is shown in Fig. 4(a). Here, the z coordinate clearly varied following the surface asperity. Note that the increasing trend came from the imperfection of sample alignment, that is, the sidewall of the line pattern was not completely parallel to the x axis of the tip scanning. Thus, the LER height distribution must be organized according to the AFM data from the z coordinate to show a horizontal cross-section against an arbitrary height. A height-constant sidewall profile was formed by points picked up from multiple fast-scan profiles and is shown projected onto the xz plane in Fig. 4(b). Here, the red strip indicates the height-constant sidewall profile, which is shown projected onto the xy plane in Fig. 4(c). No frequency filtering was applied. The sidewall profile consisted of 4449 points. The strip z width was determined such that each strip contained more than 2000 data points, i.e., the amount of sampling points of each fast-scan profile. The jagged profile shown in Fig. 4(c) indicates the sidewall roughness, not the noise of tip scanning, apparent from the clusters of points at each location along the x axis picked up from multiple fast-scan profiles. Here, the resolution of sidewall scanning in the y direction was better than 0.5 nm, which roughly corresponds to the thickness of the profile as the measurement noise.
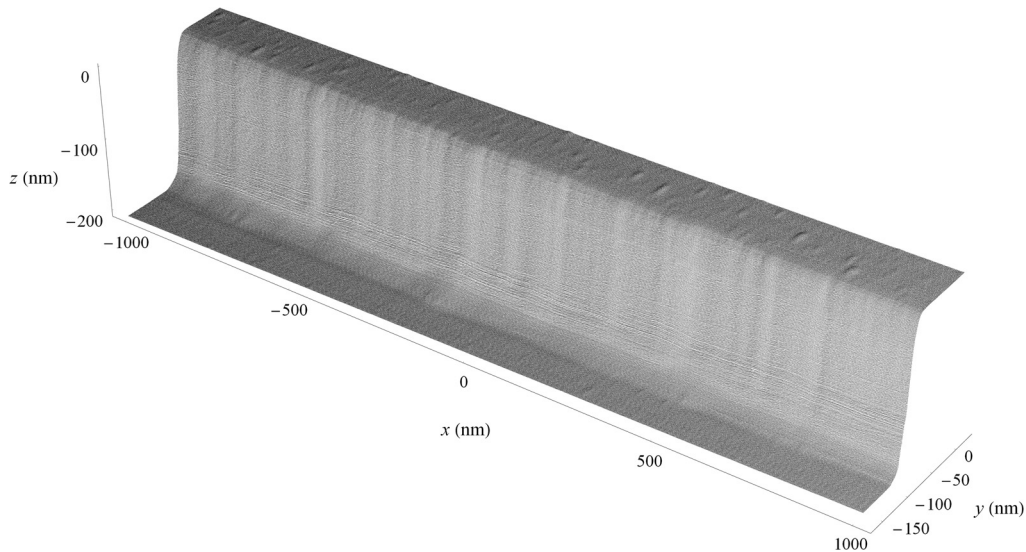
Fig. 3 AFM data of the Si line pattern measured from one side. Scale of the x axis was compressed for visibility of sidewall roughness.
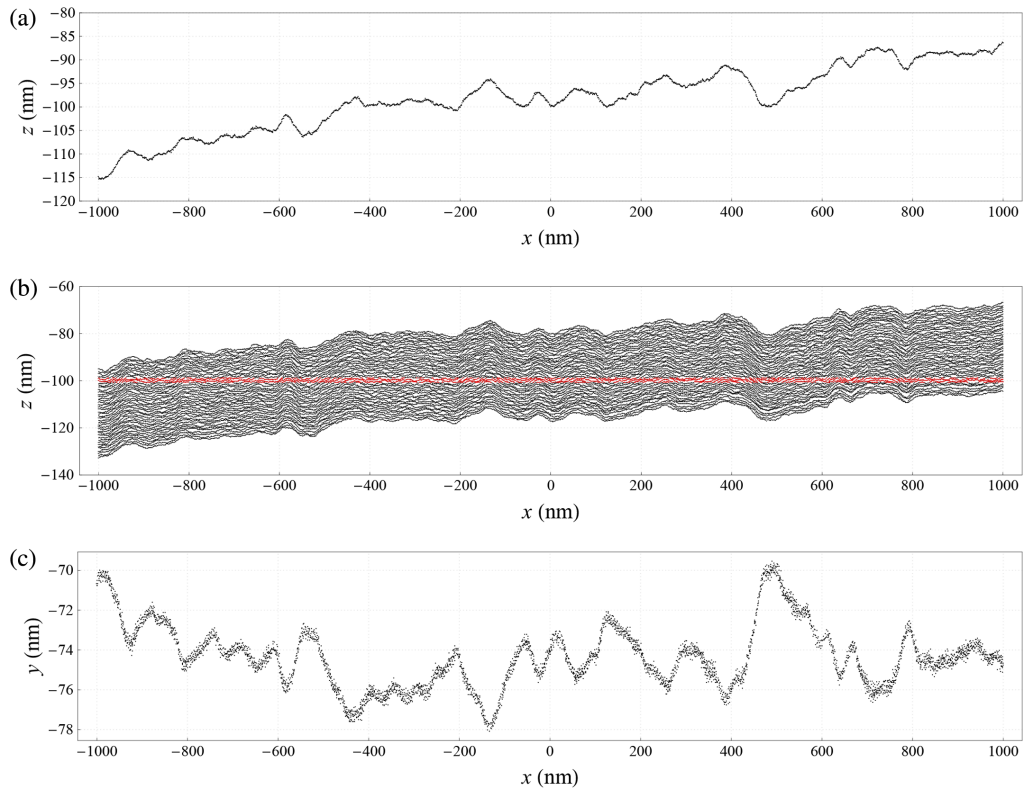

Fig. 4 (a) Projection onto the xz plane of one fast-scan profile extracted from the AFM data to observe the height variation. The height of the fast-scan profile measured on sidewall varies following the sidewall asperity. (b) Projection onto the xz plane of height-constant sidewall profile (red strip) formed by points picked up from multiple fast-scan profiles (black lines). (c) The height-constant sidewall profile [red strip in Fig. 4(b)] projected onto xy plane.

The AFM data were analyzed to calculate the LER by first defining the height of the line pattern using plane-fitting of the point clouds at the bottom and top surfaces. The point clouds at the sidewall were then divided into 100 equal-width strips, i.e., the height-constant sidewall profiles at each height were formed using the method described above (Fig. 5).
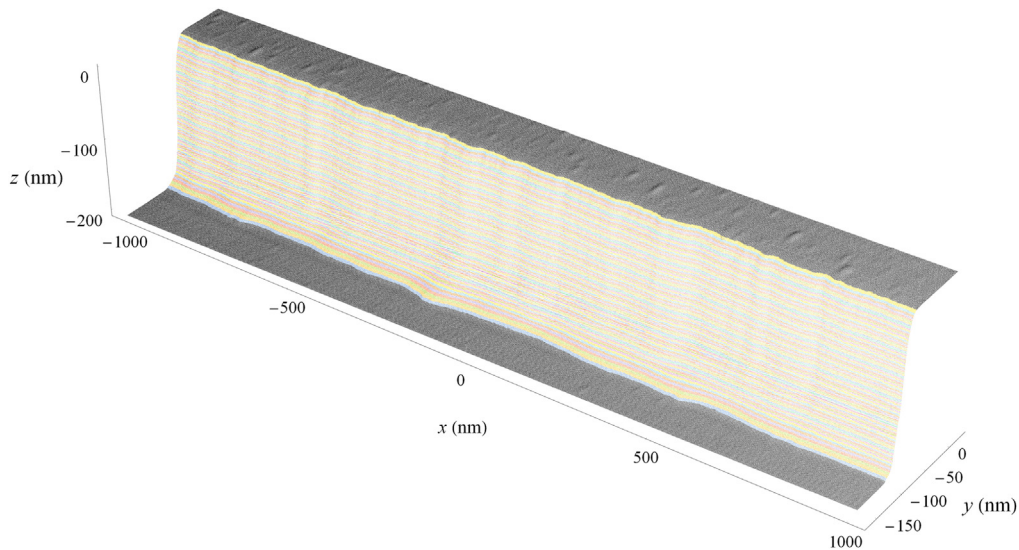
Fig. 5 Point clouds on the sidewall divided into 100 strips with equal width shown with color-coding.
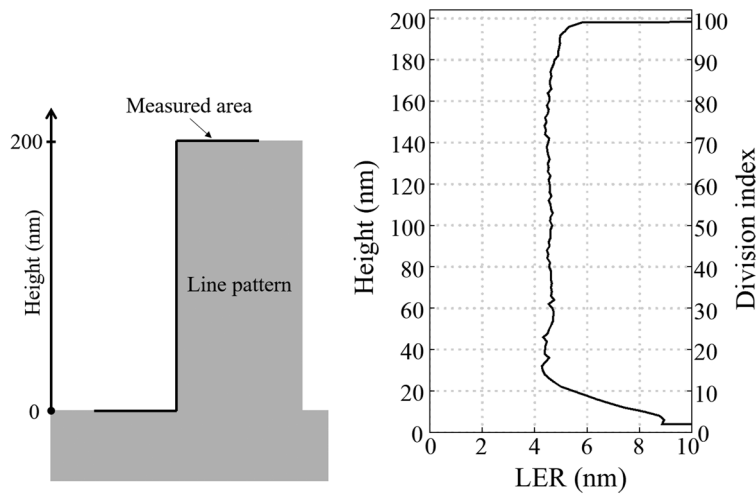
Fig. 6 LER distribution along height.

The LER was calculated as three times a standard deviation of the distance of each point from the fitted line of the points. The LER was calculated from each divided point cloud of Fig. 5. Figure 6 shows the resulting LER distribution along the height. The LER of the line pattern at the half height was 4.65 nm. Many points around the top and bottom flat surfaces fall into one strip. Therefore, the LERs around the top and bottom have large errors and are unreliable.

3.2 *Scaling Analysis of LER*

PSD and/or HHCF are often used for scaling analysis of LER,[24,25] and the roughness parameters, standard deviation (σ), roughness exponent (α), and correlation length (ξ), which characterizes the roughness profile better than solely using σ, are obtained. However, as the resolution of LER measurement using SEM is degraded by instrumental noise, the PSD in the high-frequency region is biased (forming a flat noise floor) and causes error in the LER. The flat noise floor was corrected, and the result shows good reproducibility in the previous studies,[2–4] although the precision of the measurement of roughness parameters has not yet been investigated sufficiently. We confirm the noise level of the PSD and HHCF toward reference metrology of roughness parameters and preliminarily calculate the roughness parameters from HHCF.

The point clouds of Fig. 4(c) were interpolated and resampled with a 1-nm interval, corresponding to 2000 points, to analyze the PSD and HHCF. In the PSD calculation, we use the discrete Fourier transform, $F(k)$, defined as

$$F(k_j) = \frac{1}{N} \sum_{n=0}^{N-1} x_n e^{-2\pi i n j/N},\qquad(1)$$

where $k_j = j/N$ represents the spatial frequency and x_n ($n = 0,1,2,\ldots,N-1$, N is the total number of the points and an even number) are the resampled points with a constant interval d. The PSD, $P(k_j)$, is calculated for $j = 1,2,\ldots,N/2$ because $F(k_j)$ is symmetrical about $j = N/2$

$$P(k_j) = 2d|F(k_j)|^2,\qquad(2)$$

where the factor of 2 is multiplied to keep the total power. The PSD is shown in Fig. 7(a). The HHCF, $G(r = md)$ ($m = 1,2,\ldots,N-1$), is calculated as[24]

$$G(r = md) = \left[\frac{1}{N-m} \sum_{n=1}^{N-m} (x_{n+m} - x_n)^2\right]^{1/2},\qquad(3)$$

and is shown in Fig. 7(b). Although averaging and filtering processes were not applied to the sidewall profile [Fig. 4(c)] used for the PSD calculation, the flat noise floor of the PSD detected in the high-frequency region was several orders of magnitude lower than that of a typical SEM.[2–4] The variation of the $P(k)$ increased at frequencies higher than 0.1 nm^{-1}. There was a peak at 0.259 nm^{-1} that corresponds to a wavelength of 3.86 nm. The source of these variations and peak is unclear and may be due in part to the instruments used; further investigation is
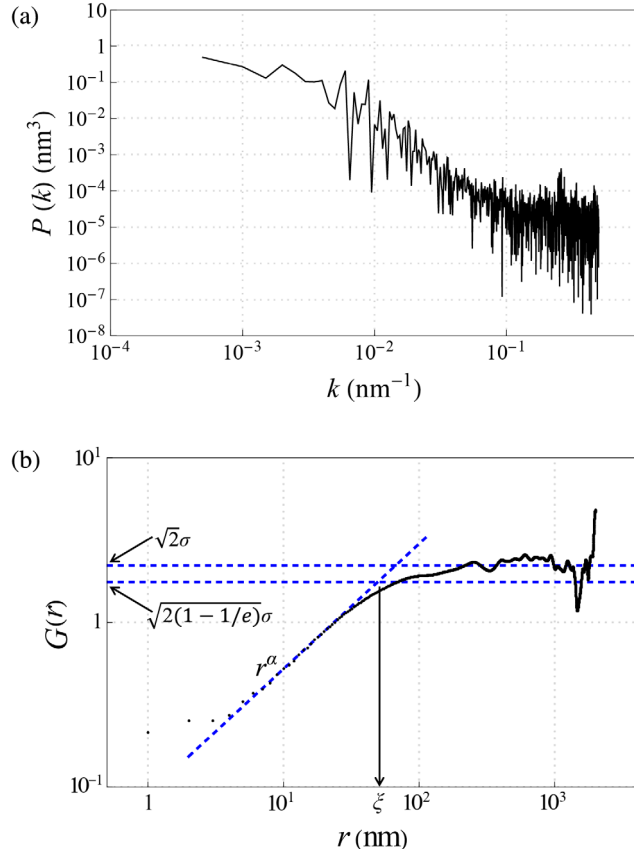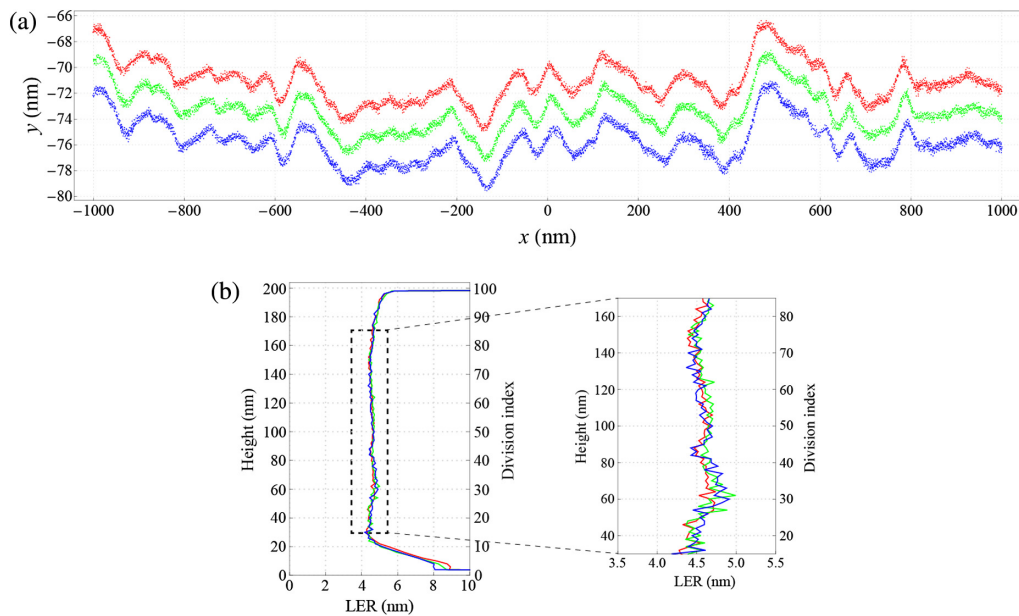

Fig. 7 (a) PSD and (b) HHCF of the sidewall profile at the half height.

Fig. 8 (a) Three sequentially measured AFM sidewall profiles at the half height projected onto the xy plane (with offsets for clarity). (b) LER distribution along the height of the three measured AFM data sets.

needed to understand this effect on LER measurement error. Roughness parameters (σ, α, and ξ) obtained from HHCF were 1.57 nm, 0.76, and 49.5 nm, respectively.

3.3 *Repeatability of LER Measurements*

Three AFM sidewall data sets were sequentially measured to evaluate the repeatability of the LER measurement; these profiles, shown in Fig. 8(a), demonstrate the high repeatability of the sidewall measurements. The LER height distribution was also calculated from the three AFM data sets and is shown in Fig. 8(b). The standard deviation of the LER at each height (index ranging from 15 to 85, leaving out the part around the bottom and top of the line pattern) of the three results was then calculated. The average and standard deviation of the calculated standard deviations at each height index were 0.07 and 0.04 nm, respectively, indicating high repeatability of the proposed LER measurement methodology.

4 Conclusion

An LER measurement technique was developed based on the tilting-mAFM technique for LER reference metrology. The sidewall profile of a line pattern was measured using tilting-tip scanning along a line pattern with high sampling density (≥ 1 nm^{-2}). The AFM data were then analyzed to divide the point cloud into 100 strips in the height direction to analyze the LER distribution along the height. The obtained line edge profile at each height showed that the resolution of sidewall scanning in the y direction was better than 0.5 nm. The calculation of the PSD and HHCF indicated that the proposed tilting-mAFM method had much lower noise than a typical SEM, although further investigation into noise in the high-frequency region in the PSD is necessary. Finally, the repeatability of the LER measurements was investigated by repeating the experiment three times. These trials indicated that the repeatability of the LER measurements, evaluated as an average of standard deviations at each height, was 0.07 nm. The proposed measurement technique is capable of nondestructive 3-D sidewall measurement with traceability to the SI unit of length and high resolution and repeatability and thus is promising for future usage in LER reference metrology. Future work will focus on investigating the calibration method of SEM's LER measurements using the tilting-mAFM technique as LER reference metrology.

5 Appendix: Dependency of Servo-Control Stability and the Measured Line Edge Profile on θ_p

A higher inclining angle of the servo axis, θ_p, enables a higher data density on the sidewall[22] and is preferable. On the other hand, an angle of θ_p that exceeds a certain threshold makes the inclining-servo-control unstable and causes high noise in the line edge profile. We investigated the θ_p-dependency of the line edge profile by repeatedly measuring the same location with different θ_p. Figure 9(a) shows line edge profiles at the half height measured with different θ_p. Figure 9(b) shows θ_p-dependency of repeatability of the fast scan in the x, y, and z coordinates on the sidewall investigated in the same way as Table 1. Figure 9(c) shows HHCFs calculated from line edge profiles in Fig. 9(a).

In Fig. 9(a), the line edge profiles of 45 deg and 60 deg are noisier than those of 15 deg and 30 deg. This is consistent with the repeatabilities in the y axis of 45 deg and 60 deg being much higher than those of 15 deg and 30 deg as shown in Fig. 9(b). Note that, except for the noise level, these four profiles have almost the same shape that indicates the θ_p-dependency of the profile shape is small. Figure 9(c) shows that HHCFs of 15 deg and 30 deg have low noise and similar shape, resulting in almost the same roughness parameters. Therefore, we conclude that an angle approximately between 15 deg and 30 deg is suitable for θ_p in the LER measurement.
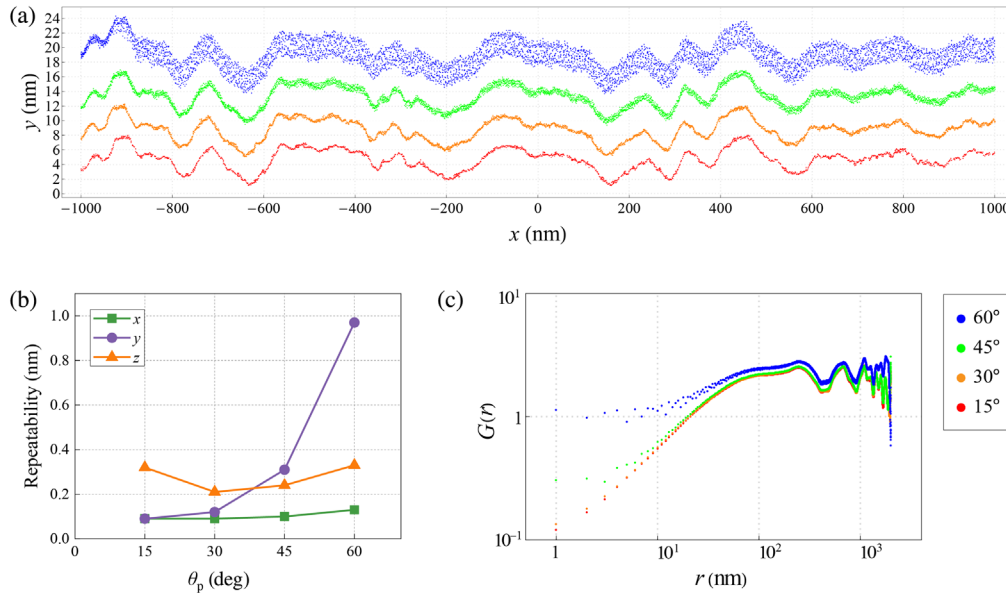
Fig. 9 (a) Line edge profiles at the half height measured with different θ_p (red: 15 deg, orange: 30 deg, green: 45 deg, and blue: 60 deg), with offsets to clarify comparing them. (b) Repeatability of the fast scan in the x, y, and z coordinates on the sidewall with different θ_p. (c) HHCFs calculated from the line edge profiles with different θ_p (red: 15 deg, orange: 30 deg, green: 45 deg, and blue: 60 deg).

Acknowledgments

References

1. J. S. Villarrubia et al., "Dimensional metrology of resist lines using a SEM model-based library approach," *Proc. SPIE* **5375**, 199 (2004).

2. J. S. Villarrubia and B. D. Bunday, "Unbiased estimation of linewidth roughness," *Proc. SPIE* **5752**, 480–488 (2005).

3. L. Azarnouche et al., "Unbiased line width roughness measurements with critical dimension scanning electron microscopy and critical dimension atomic force microscopy," *J. Appl. Phys.* **111**, 084318 (2012).

4. G. F. Lorusso et al., "Unbiased roughness measurements: subtracting out SEM effects," *Microelectron. Eng.* **190**, 33–37 (2018).

5. N. G. Orji et al., "Metrology for the next generation of semiconductor devices," *Nat. Electron.* **1**, 532–547 (2018).

6. A. Cordes et al., "Towards development of a sidewall roughness standard," *Proc. SPIE* **8681**, 86812J (2013).

7. G. F. Lorusso et al., "Line width roughness accuracy analysis during pattern transfer in self-aligned quadruple patterning process," *Proc. SPIE* **9778**, 97780V (2016).

8. K. Takamasu et al., "3D-profile measurement of advanced semiconductor features by using FIB as reference metrology," *Proc. SPIE* **10145**, 101451A (2017).

9. H. Kawada et al., "How to measure a-few-nanometer-small LER occurring in EUV lithography processed feature," *Proc. SPIE* **10585**, 1058526 (2018).

10. K. Takamasu et al., "Linewidth roughness of advanced semiconductor features using focused ion beam and planar-transmission electron microscope as reference metrology," *J. Micro/Nanolith. MEMS MOEMS* **17**(4), 041010 (2018).

11. P. Faurie, J. Foucher, and A.-L. Foucher, "The LER/LWR metrology challenge for advance process control through 3D-AFM and CD-SEM," *Proc. SPIE* **7520**, 75200F (2009).

12. V. A. Ukraintsev et al., "SI-traceable calibration of linewidth roughness of 25 nm nanoCD standard," *Proc. SPIE* **7638**, 76383U (2010).

13. M. Fouchier, E. Pargon, and B. Bardet, "An atomic force microscopy-based method for line edge roughness measurement," *J. Appl. Phys.* **113**, 104903 (2013).

14. N. G. Orji et al., "Line edge roughness metrology using atomic force microscopes," *Meas. Sci. Technol.* **16**, 2147–2154 (2005).

15. G. Dai et al., "Development of a 3D-AFM for true 3D measurements of nanostructures," *Meas. Sci. Technol.* **22**, 094009 (2011).

16. S.-J. Cho et al., "Three-dimensional imaging of undercut and sidewall structures by atomic force microscopy," *Rev. Sci. Instrum.* **82**, 023707 (2011).

17. Y. Hua et al., "High throughput and non-destructive sidewall roughness measurement using 3-Dimensional atomic force microscopy," *Proc. SPIE* **8324**, 83240I (2012).

18. J. Foucher et al., "Introduction of next-generation 3D AFM for advanced process control," *Proc. SPIE* **8681**, 868106 (2013).

19. H. Xie et al., "Atomic force microscope caliper for critical dimension measurements of micro and nanostructures through sidewall scanning," *Ultramicroscopy* **158**, 8–16 (2015).

20. D. Hussain et al., "Atomic force microscopy sidewall imaging with a quartz tuning fork force sensor," *Sensors* **18**, 100 (2018).

21. F. Chouchane et al., "Sub-10 nm plasma nanopatterning of InGaAs with nearly vertical and smooth sidewalls for advanced n-fin field effect transistors on silicon," *J. Vac. Sci. Technol. B* **35**, 021206 (2017).

22. R. Kizu et al., "Development of a metrological atomic force microscope with a tip-tilting mechanism for 3D nanometrology," *Meas. Sci. Technol.* **29**, 075005 (2018).

23. R. Kizu et al., "Linewidth calibration using a metrological atomic force microscope with a tip-tilting mechanism," *Meas. Sci. Technol.* **30**, 015004 (2019).

24. A. Yamaguchi and O. Komuro, "Characterization of line edge roughness in resist patterns by using Fourier analysis and auto-correlation function," *Jpn. J. Appl. Phys.* **42**, 3763–3770 (2003).

25. V. Constantoudis et al., "Quantification of line-edge roughness of photoresists. II. Scaling and fractal analysis and the best roughness descriptors," *J. Vac. Sci. Technol. B* **21**, 1019–1026 (2003).

26. R. Kizu et al., "Accurate vertical sidewall measurement by a metrological tilting-AFM for reference metrology of line edge roughness," *Proc. SPIE* **10959**, 109592B (2019).

Ryosuke Kizu is a researcher at the National Metrology Institute of Japan, National Institute of Advanced Industrial Science and Technology. He received his BS and MS degrees in engineering from Nagoya University in 2013 and 2015, respectively. His current research interests include dimensional nanometrology, nanoscale calibration standards, and development of a metrological AFM.

Biographies of the other authors are not available.